Available online at www.CivileJournal.org

Civil Engineering Journal

(E-ISSN: 2476-3055; ISSN: 2676-6957)

Vol. 11, No. 02, February, 2025

Flexural Behaviour of Precast Lightweight Concrete Sandwich Slabs With Demountable Bolted Steel Shear Connectors

Rana H. Al-Kerwei [1, 2*], S. A. Osman [2], Ahmed W. Al-Zand [2, 3], Ammar N. Hanoon [4]

[1] Department of Civil Engineering, Mustansiriyah University, Baghdad, Iraq.

[2] Department of Civil Engineering, Universiti Kebangsaan Malaysia (UKM), Bangi 43600, Selangor, Malaysia.

[3] Department of Design, College of Fine Arts, Al-Turath University, Baghdad, Iraq.

[4] Department of Reconstruction and Projects, University of Baghdad, Baghdad 10071, Iraq.

Received 25 October 2024; Revised 17 January 2025; Accepted 21 January 2025; Published 01 February 2025

Abstract

A concrete slab is a fundamental element and contributes the highest weight in structural buildings. In this paper, a new type of sandwich slab consisting of two layers of lightweight concrete and demountable steel connectors is proposed in a new attempt to reduce the weight of the floors within the structure and apply a simpler and faster approach to connecting the layers of sandwich panels. The structural effects of the proposed connectors on Precast Lightweight Concrete Sandwich Slab (PLCSS) are evaluated experimentally and theoretically in terms of strength, stiffness, degree of composite action, and usability for floor construction. The behaviors of six PLCSS specimens subjected to four-point loads were investigated, studying the effects of varied parameters such as different numbers, arrangements, and shapes of demountable steel connectors (I, V, and X connector shapes) fastened with steel bolts, in addition to one solid concrete slab as a reference specimen. The panels' performance in this structural system was evaluated by measuring the degree of composite action using load, displacement, stress, and neutral axis methods. Based on the experimental results, the slab panels exhibited composite panel behavior until the point of failure. Under flexural loads, the panel behaved similarly to that of a solid one-way slab; crack patterns appeared in one direction. The specimens with IC, VC, and XC showed different load capacity values, ranging from 22.74 kN to 50.55 kN; these values depend on the types of shear connectors and their numbers in the sandwich panels. Using V and X connectors enhances the composite action between layers, increasing the shear demand and making the shear failure more likely. It can be concluded that demountable shear connectors can transfer shear between the two concrete wythes, resulting in a composite panel with structural integrity, a lighter weight, and satisfying ACI specifications for floor applications.

Keywords: Demountable Connectors; Sandwich Slab; Degree of Composite Action; Flexural Behavior; Composite Slab.

1. Introduction

The incredible rate of population rise, particularly in developing countries, has intensified the need for infrastructural facilities, natural resources, and energy, leading to considerable stress on the environment and biosphere. Sustainability has grown to be an imperative concept in solving the escalating challenges associated with rapid economic and population growth. The achievement of sustainability is directly related to the design, construction, and operation of the structural system that reduces the use of resources, eliminates the environmental effects, and improves the long-term effectiveness. Rapid building techniques like precast and composite construction might meet this massive infrastructure

* Corresponding author: p115460@siswa.ukm.edu.my

http://dx.doi.org/10.28991/CEJ-2025-011-02-06

need and the sustainability requirements. Because of its mechanized industrial setup, the precast building allows for quick construction, cost savings on a large scale, and quality control. In the construction industry, precast technology and lightweight structural members have gained widespread popularity. The features of precast technology and lightweight structural components are combined in precast concrete sandwich panels.

A sandwich panel is a composite construction of three layers (wythes): a core layer with low density sandwiched between two thin skin layers, which are connected using connectors. The panels' composite action may be produced by connecting the wythes with discrete or continuous shear connectors made of wires or steel rebars [1]. The structural performance of sandwich panels depends on the stiffness and strength of each concrete layer and the composite interaction between them, which is achieved by the presence of shear connections. Sandwich panels are used in applications where a combination of high structural rigidity and low self-weight is required by using a lightweight and thick layer for the core and strong but thin layers for the face layers. As a result, the overall thickness of the plate increases, enhancing structural features such as bending stiffness with less self-weight.

Precast Concrete Sandwich Slab (PCSS) represents a significant portion of the cost and weight of precast concrete structures. Information on precast concrete sandwich slabs can be found in many studies [2–4]. Due to the reduced volume of concrete, the sandwich slabs are lighter than solid slabs of comparable strength. Because most of these panels are precast, their lighter weight is advantageous for shipping and construction. The weight decrease significantly impacts the cost associated with these panels. So, the weight of PCSP can be reduced even more to make them suitable for a wider variety of structures by using lightweight concrete, which has lately emerged as a promising solution for replacing standard concrete in the construction industry due to their lower cost and higher thermal and structural efficiency. At the same time, it contributes to green building by producing a cleaner and more orderly environment on the job site and a shorter total construction timeline [5].

Shear connectors are crucial for concrete sandwich panels' structural and thermal efficiency. Their design, material, and connection method substantially influence the efficiency of the concrete panels; various materials with different strengths and conductivity were used in sandwich panels, such as steel [6–8], GFRP [9, 10], FRP [11–13], BFRP [14, 15], and Steel Glass Fiber-reinforced Polymer (SGFRP) [16]. Einea et al. [17] classified connectors as one-way or two-way depending on their geometric shape. The one-way connector is always designed to transfer one-way in-plane shear force, and its performance in the two orthogonal directions is different. On the other hand, the performance of a two-way connector is the same in both directions, and it can be designed to transfer in-plane shear in both directions. The connectors can be further divided into two types based on their shapes: continuous, which include the C-ties, M-ties, and Z-ties, and discrete or non-continuous connectors, such as bent wire, truss-shaped, and grid-type connectors [18]. Recently, many studies have been conducted on the performance of PCSPs with different forms of shear connectors: corrugated GFRP shear connectors [19], GFRP pin [16, 18], W-shaped SGFRP and W-shaped GFRP [16], steel bar in the shape of trusses [20, 21], GFRP pin connectors in a star pattern [22], truss grid CFRP [11, 23], steel truss [2, 4, 16], steel stud [3, 24], a combination of plate-type shear connectors and pin-type shear connectors [6], flat plate, a corrugated plate, and a hexagonal tube GFRP connectors [25], X-shaped GFRP bar [9, 10, 26], steel bent bars [27], steel plate connectors [7, 28], Z-shaped steel plate connector [29], hexagonal tubular and the plate- type FRP connectors [13, 30], inclined bar welded with top and bottom wire mesh [31], wide-flanged cross-section with 4, 3, and 2 legs from different reinforced and unreinforced polymer types [32], BFRP diagonal bar [15], FRP grid connector [33], and rectangular and cross-section FRP [12]. The type and arrangement of shear connectors affect the degree of composite action of the sandwich panels, depending on the level of shear force transmitted between their layers, as shown in Figure 1 [10]. Lighter and more structurally efficient members were typically the result of high levels of composite action.

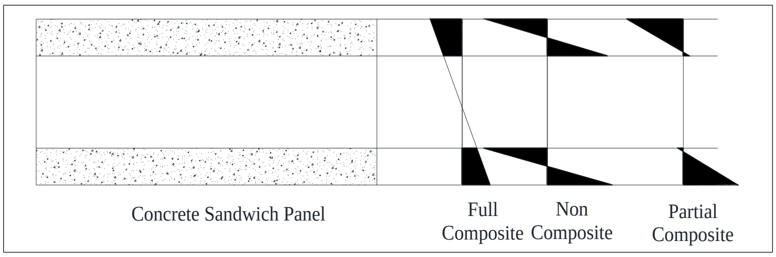

Figure 1. Approximate Strain Distribution for Full, Non, and Partial Composite Behaviours

To enhance structural integrity while reducing the economic and environmental costs associated with the production of concrete sandwich panels by providing easier and faster methods of connection, Alfeehan & Sheer [3] developed and evaluated a structural system that may be employed in precast concrete by pouring each layer separately and then connecting them with each other by mechanical connectors. Thus, these parts can be supplied in quantities as needed in the factory and then transported and installed on the job site, in addition to controlling the thickness of the sandwich panel; therefore, further research on other types of shear connectors is necessary to evaluate the degree of composite action between the layers. The difficulty of fixing the connectors when the panel's dimensions are large is one of the main disadvantages of the connectors employed in the subsequent linking method, so it is essential to improve this method by using other types of connectors.

In composite bridges, the study of subsequent linking methods for steel shear connectors, which include the demountable types, has undergone substantial progress in recent times, and many studies have investigated the behaviors of demountable shear connectors in sustainable composite beams [34–38]. Utilizing demountable connectors is an advanced technical solution that improves structural integrity. Its user-friendly nature simplifies the connection of both old and new structural components through the ability to disassemble, reconnect, and assemble the structural elements. These connections generally use mechanical fastening devices like bolts or other replaceable fasteners. Steel bolts are widely utilized as fasteners in steel structures due to their impressive characteristics, such as superior fatigue performance, intense connection, and ease of disassembly [34]. Using demountable connectors with subsequent linking methods may help produce sandwich panels with adequate composite action and easy layer connection with reuse possibility.

To date, all studies have been conducted on the bolted shear connectors in composite beams only. Therefore, this study investigates the feasibility of using these shear connectors in precast lightweight concrete sandwich slabs as sustainable structural elements and evaluates their structural behavior. The structural strength characteristics of small-scale PLCSS under a four-point load with foamed concrete wythes are thoroughly researched, the degree of composite action (DCA) is evaluated, and the suitability of using PLCSS with demountable shear connectors as a slab element is investigated. The composite effects are assessed using test findings focusing on crack patterns, load-displacement relationships, and strain distributions. Figure 2 presents the methodology of the present work.

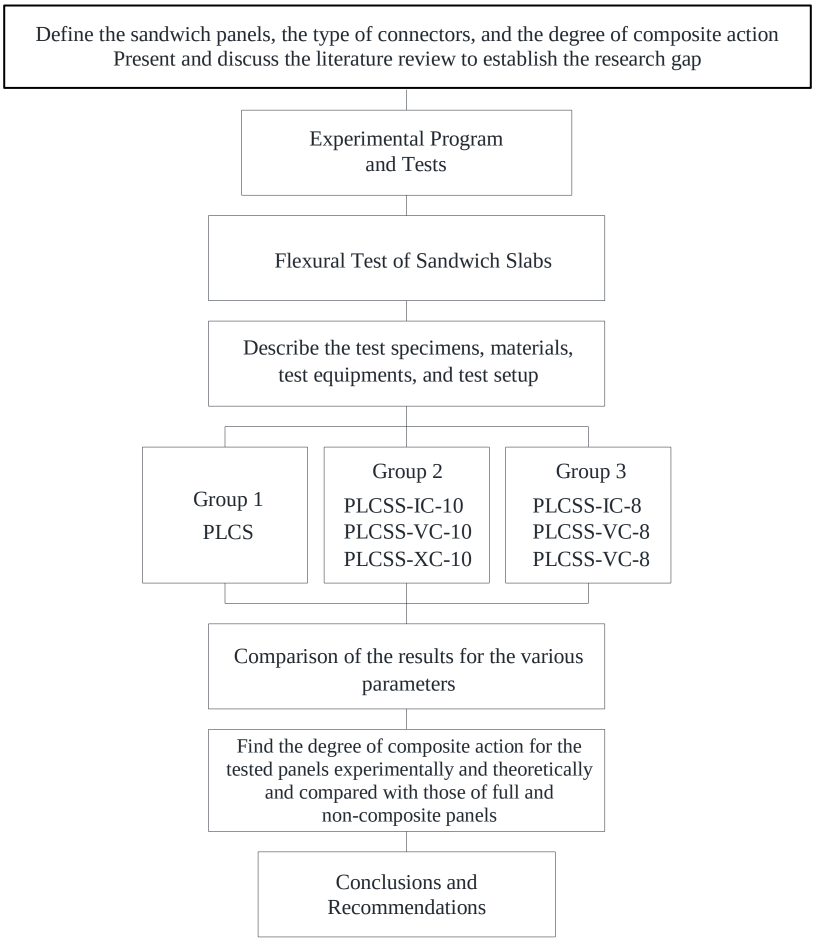

Figure 2. Methodology of the Study

2. Experimental Program

The most challenging issue often faced by researchers is how to achieve the integrity of sandwich panels and guarantee a strong connection between their layers. The present experimental study investigates the effect of three different types of demountable bolted steel shear connectors: I connectors with two bolts in each connector, V connector with three bolts in each connector, and X connector with four bolts in each connector on flexural behavior of PLCSS. The parameters in this study are the type, number, and arrangement of connectors. Seven small scale lightweight specimens, divided into three groups as summarized in Table 1, were tested at the Laboratories of the Materials and Structures of the College of Engineering at Mustansiriyah University. The tests aimed to provide information about the general behavior and suitability for the practical application of sandwich panels with demountable steel connectors.

Table 1. Configurations of Panels

Group	ID[a]	Type of Shear Connector	No. of Shear Connector	Layout of Shear Connector	A_s[b] (mm^2)	A_s, min[c] (mm^2)
1	PLCS	×	×	×	157	129
2	PLCSS-IC-10	I Connector	10	1	157	129
	PLCSS-XC-10	X Connector	10	1	157	129
	PLCSS-VC-10	V Connector	10	1	157	129
3	PLCSS-IC-8	I Connector	8	2	157	129
	PLCSS-XC-8	X- Connector	8	2	157	129
	PLCSS-VC-8	V- Connector	8	2	157	129

[a] PLCS: Precast Lightweight Concrete Slab; PLCSS: Precast Lightweight Concrete Sandwich Slab; TC, XC, VC: Tube Connector, X Connector, V Connector. 10, 8: Number of Connectors in the specimen; [b] Ø5 mm dia. wires at 50 mm c/c; [c] Based on ACI 318-19.

2.1. Sandwich Slab Specimens

Six small-scale PLCSS with dimensions (L=1200×W=400) mm and each concrete layer was set at H=40 mm to provide the minimum thickness requirements for durability and fire resistance with 100 mm of insulation layer and one solid PLCS with dimensions (L=1200, W=400, and H=180) mm were tested under four-point loading. The layer arrangement, thickness, and reinforcement ratio were chosen to imitate the sandwich slab previously designed in accordance with the ACI-318 code. Figure 3 shows a schematic sketch of the concrete specimens used in the present study. The details of solid and sandwich slabs are given in Table 1. The dimensions of demountable steel connectors were chosen to be equal to each other in terms of contact area with concrete and arranged along the panel's span. The panel's effective moment resistance is limited to the span direction. The dimensions and details of the demountable steel shear connectors are shown in Figures 4 and 5.

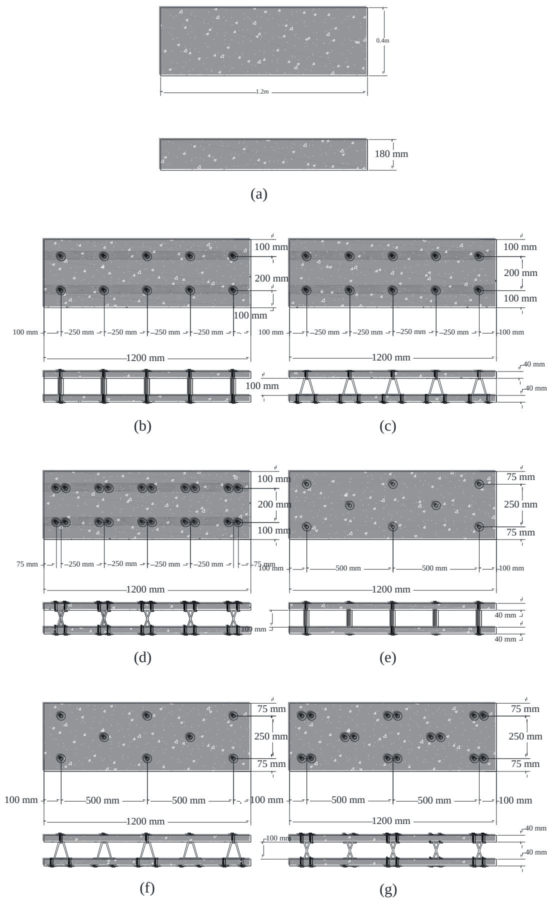

Figure 3. Schematic Sketch of Top and Side View for: (a) PLCS (b); PLCSS-IC-10; (c) PLCSS-VC-10; (d) PLCSS-XC-8; (e) PLCSS-IC-8 ; (f) PLCSS-VC-8; (g) PLCSS-XC-8

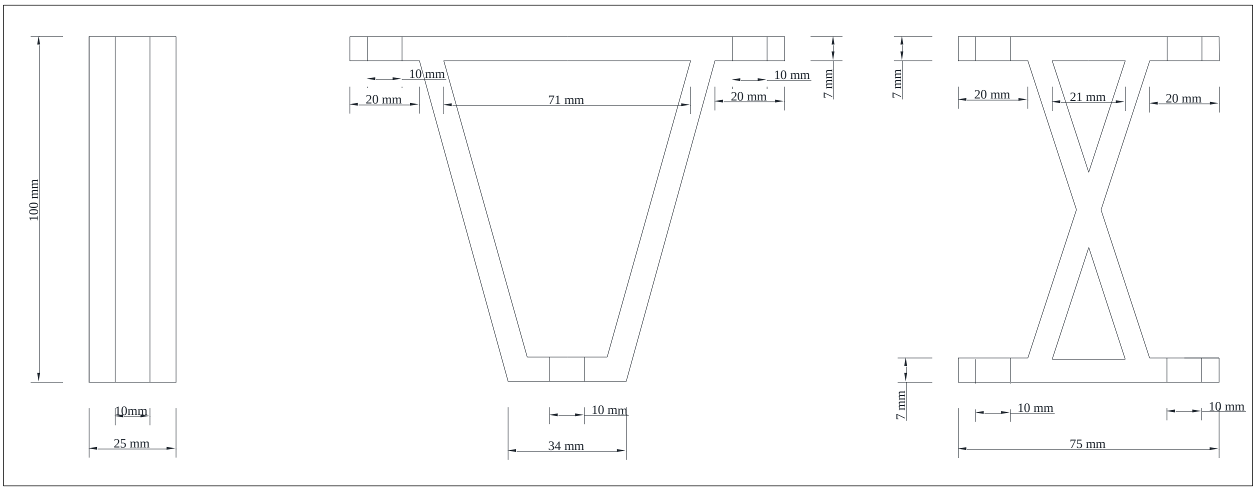

Figure 4. Dimensions of Demountable Shear Connectors

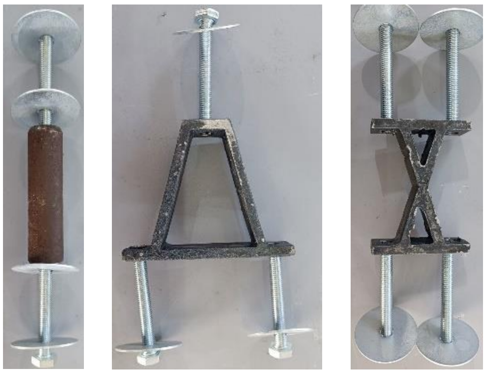

Figure 5. Bolted Shear Connectors

2.2. Materials

Lightweight foamed concrete was used to cast the sandwich panel specimens. The mix proportion of the lightweight concrete used in this investigation was proposed by Abdulkareem & Alfeehan [39] as shown in Table 2. Type 1 of ordinary Portland cement manufactured in Iraq was used to cast specimens. Natural sand of Al-Ekhaider within the Iraq Specification No.45/2021[40] requirement, as shown in Figure 6, was used as fine aggregate. The I-Connectors were made of a steel tube that was threaded inside and had outer and inner diameters of 25 mm and 10 mm, while the X and V-Connectors were made from steel plates with a thickness of 8 mm. The steel connectors were manufactured using plasma techniques based on computer-aided design. Welded steel wires were used as reinforcement for the concrete layers with a diameter of 5 mm and a spacing of 50 × 50 mm c/c. The average yield strength of steel wires was 685 MPa according to ASTM A1064 [41]. The steel bolts utilized to fasten the connectors with concrete panels had an average yield strength of 433.2 MPa, according to ASTM F593 [42]. The average test results of the hardened concrete control specimens were 1790 kg/m^3 for density, 22.84 GPa for modulus of elasticity, 25 MPa for cylinder compressive strength with a coefficient of variation of 3.3%, and 2.39 MPa for flexural tensile strength with a coefficient of variation of 9.6%.

Table 2. Mix Proportion of Lightweight concrete [39]

Material	Quantity
Portland Cement Type I	800 kg/m^3
Sand (passing through a 600-micron sieve)	800 kg/m^3
Silica Fume (0.2 micron) (8%) of Cement wt.	64 kg/m^3
Limestone (95% pass through sieve 138 µmm)	320 kg/m^3
w/c	33%
Superplasticizer (1.065 kg/liter) (2%) of Cementitious Materials	16.22 L
Aluminum Powder (0.003 of cement wt.)	2.4 kg

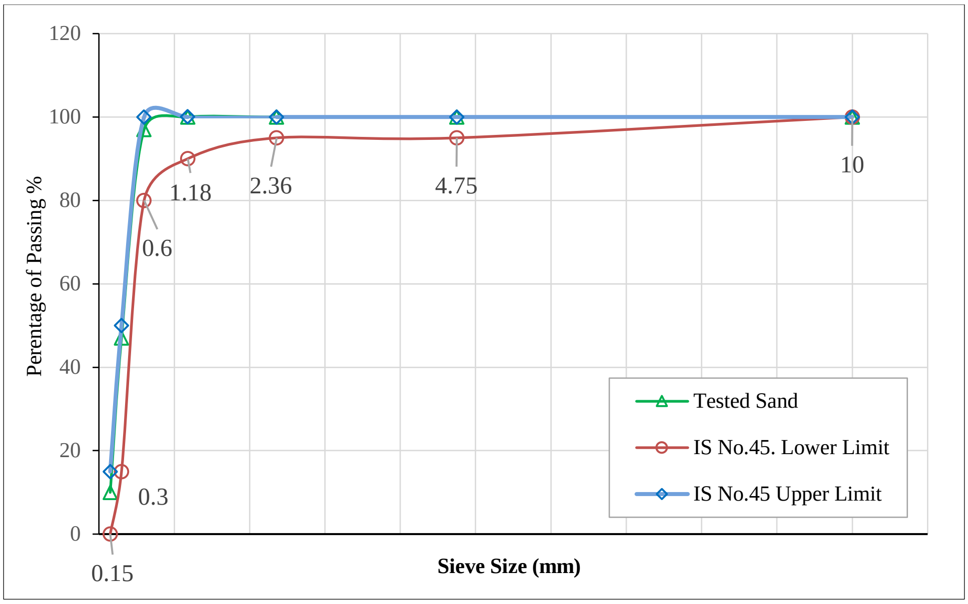

Figure 6. Grading Curve for Sand

2.3. Fabrication of Specimens

To ensure the accuracy of the shear connector locations and the straightness of their connection between the concrete layers, the steel plates used in the manufacture of each mold for each type of sandwich panel were perforated according to the previously specified measurements, resulting in a perfect match in the hole centers between the layers. Then, 8 mm studs were inserted into the holes and welded from the back of the mold. After all studs were installed, they were covered with 11 mm plastic tubes with an outer diameter slightly larger than the bolt that would fasten the shear connector to the concrete layer. The oiled plastic pipes make it easier to remove the concrete layer from the mold and keep it from adhering to the mold's studs. They also provide the eventual diameter of the hole.

The molds are placed on a flat surface, and the wire meshes are installed in their designated positions in the mid-height of the concrete layer. Lightweight concrete is poured to form the layers of sandwich panels of 40 mm thickness. The specimens are cured for 28 days. The process of connecting concrete layers to form the sandwich panels is carried out by placing the connectors in their positions and then fixing them with bolts and washers. The process of specimen fabrication is illustrated in Figure 7.

Figure 7. Process of Specimens Fabrication

2.4. Test Setup

Each panel was centered with regard to the load cell and placed at the designated position on the supports. All specimens were tested and put in the same direction as they were cast, where the rough surfaces of the outer layers were inward. With a span of 1100 mm, the sandwich slabs were simply supported by steel rollers. A four-point bending loading setup was used to test the sandwich slab specimens, as shown in Figure 8. Two steel cylinders in touch with the top surface throughout the width of the slab's cross-section were used to apply the load through hydraulic universal machines capable of 300 kN (for testing the sandwich slab) and 30000 kN (for testing the solid slab). Two rigid transfer cylinders were used to apply two-line loads to the slab. Deflections and slip were measured by Linear Variable Differential Transformers (LVDTs) affixed to an additional magnetic steel piece at the ends and mid-span of the sandwich slab; one LVDT was vertically located at the mid-span for measuring deflection (LVDT 1 with a stroke of ±50 mm), and two LVDTs were horizontally placed at the mid-depth of the upper and lower layers of concrete sandwich slabs to measure relative slip between them (LVDTs 2 and 3 with a stroke of ±10 mm). The strains were measured at the middle span of the slab using six bonded electrical strain gauges, with gauge length and resistance of 100 mm and 120 ± 0.3 Ω, respectively, at the top, bottom, and at distances of 10, 30, 150, and 170 mm from the top surface of the slab. A monotonic static load was gradually applied at a 5 kN/min rate. The failure load is determined when the top or bottom layer breaks excessively, and the applied load decrease with increasing in the deflection. The loading, vertical deflection, horizontal displacement, and strain values are recorded and saved in a computerized system.

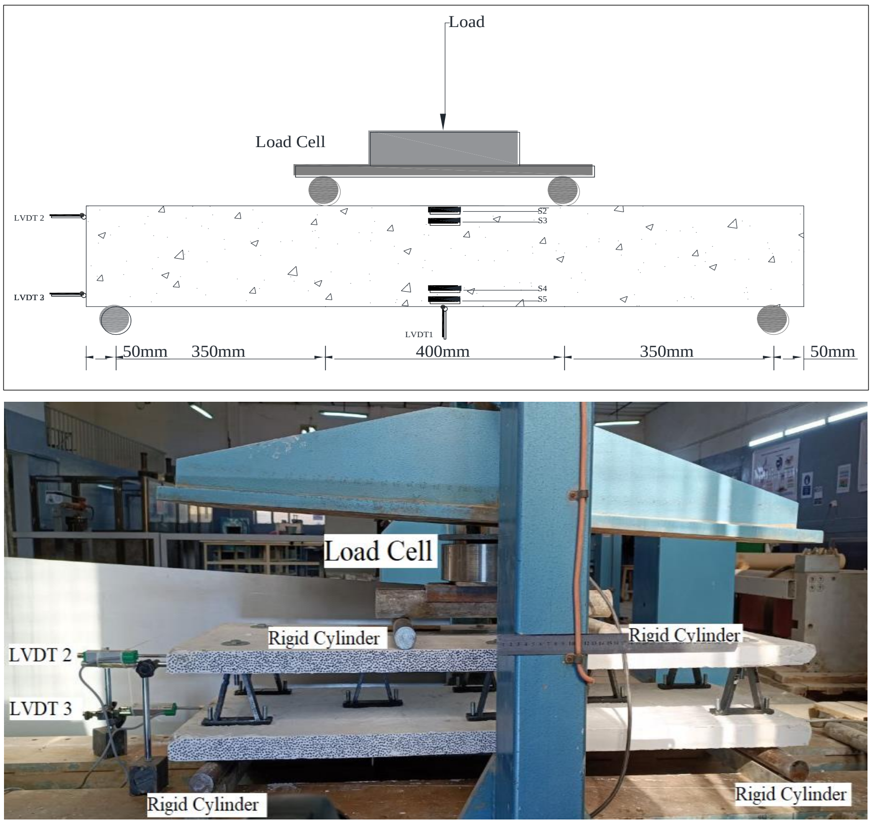

Figure 8. Loading Points and Positions of Strain and Displacement Sensors

3. Results and Discussion

In this section, the main results of the tests carried out on sandwich slabs are analyzed in the context of load-deflection relation and strain vibration across the slab depth.

3.1. Load–Deflection Relationship

The load-deflection curves obtained from flexural tests indicate that the type and number of demountable steel connectors affect the load-deflection response of concrete sandwich slabs, as shown in Figures 9 and 10. Table 3 summarizes the maximum applied load, maximum midspan deflection, and cracking load that were obtained experimentally for each specimen. In these tests, the first crack load is the load at which the first crack is seen and is inferred from the load-deflection relationship. Since the weights of the steel cylinders and specimens have a negligible effect on the overall response of the panels, it is neglected. Similar responses were shown by the sandwich slabs with I, X, and V connectors. The response curve generally consists of an initial branch until the first crack occurs, at which point the specimen's initial stiffness decreases. The panel deflected elastically, and the load-deflection was approximately linear until the first crack. After the specimens reached the ultimate load, drops in the load carrying capacity were found. The first crack load and initial stiffness for specimen PLCSS-XC-10 is the highest value; this observation may be attributed to the total number of bolts and spacing between them in the specimens, which can help to distribute the load more uniformly and reduce the stress concentration so that these sandwich slabs could deflect less with higher value of the ultimate load. The specimens PLCSS-IC-8 and PLCSS-XC-10 showed different load capacity values, ranging from 22.74 kN to 50.55kN; these values depend on the types of shear connectors and their numbers in the sandwich panels. The results showed the highest values of maximum carrying capacity for specimens with X connectors compared to others due to the highest number of bolts in the specimens. The maximum carrying capacity increased with the number of connectors for each type. The increase in the number of shear connectors from 8 to 10 connectors causes a 17.7% increase in the load capacity for specimens with I connectors, 8.66% in specimens with V connectors, and 17.66% for specimens with X connectors. The form of the connector and the contact area with the concrete layers significantly affect the structural behavior of sandwich panels. The V and X connectors have larger contact areas than those of I connectors. A wider contact area allows for improved load distribution, which leads to better composite action, enhances the structural ability to sustain load, and improves stiffness, allowing the section to withstand higher loads without excessive deformation.

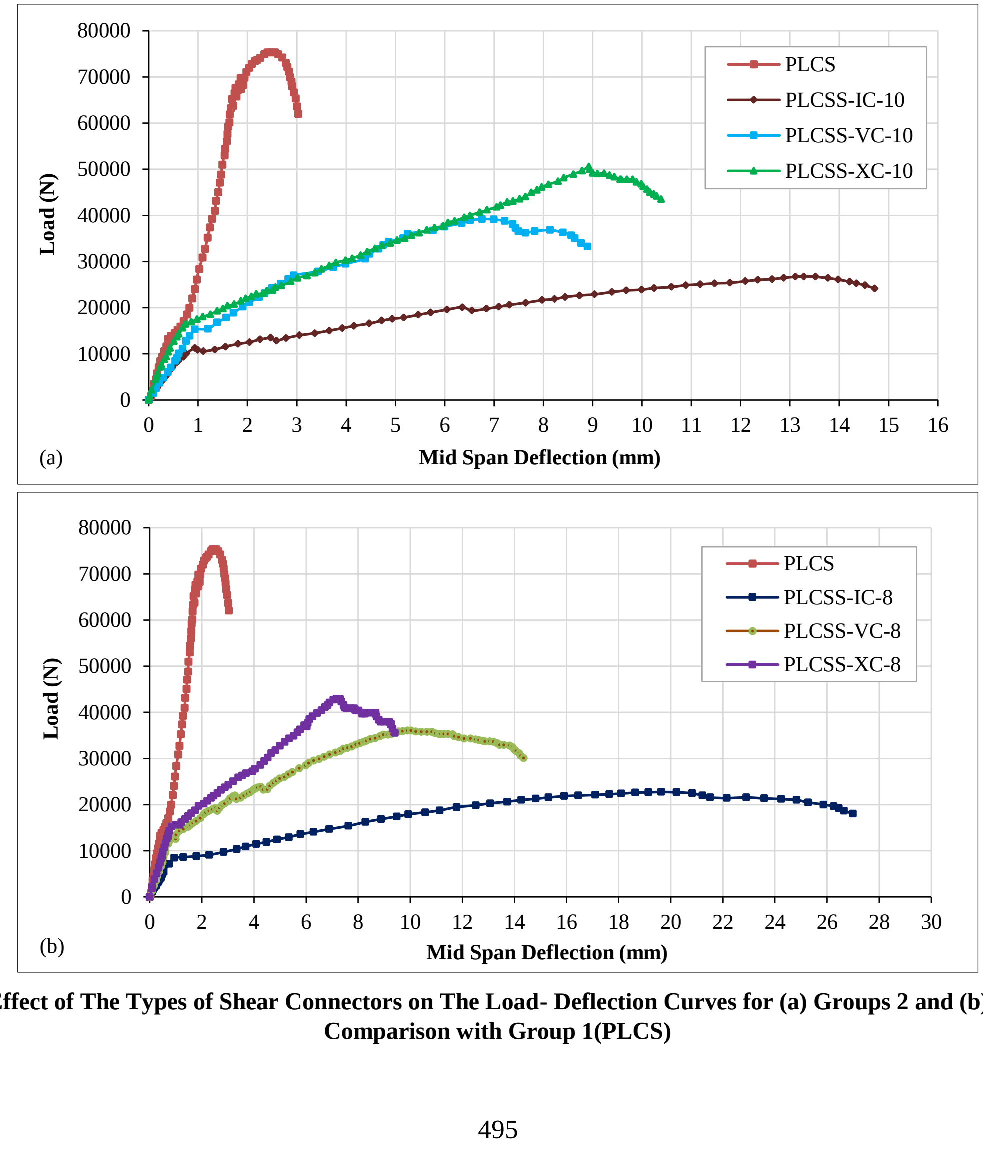

Figure 9. Effect of The Types of Shear Connectors on The Load- Deflection Curves for (a) Groups 2 and (b) Group 3 in Comparison with Group 1(PLCS)

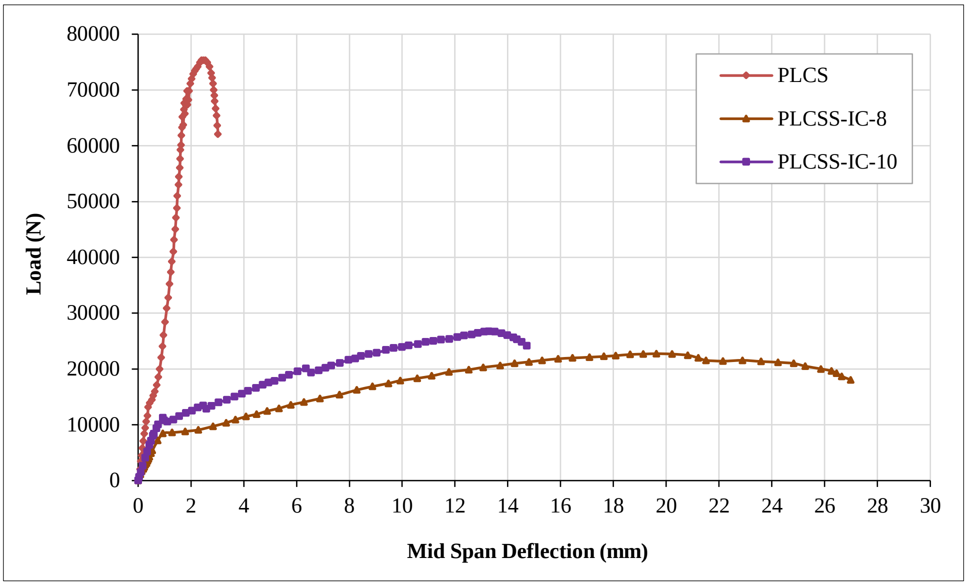

(a)

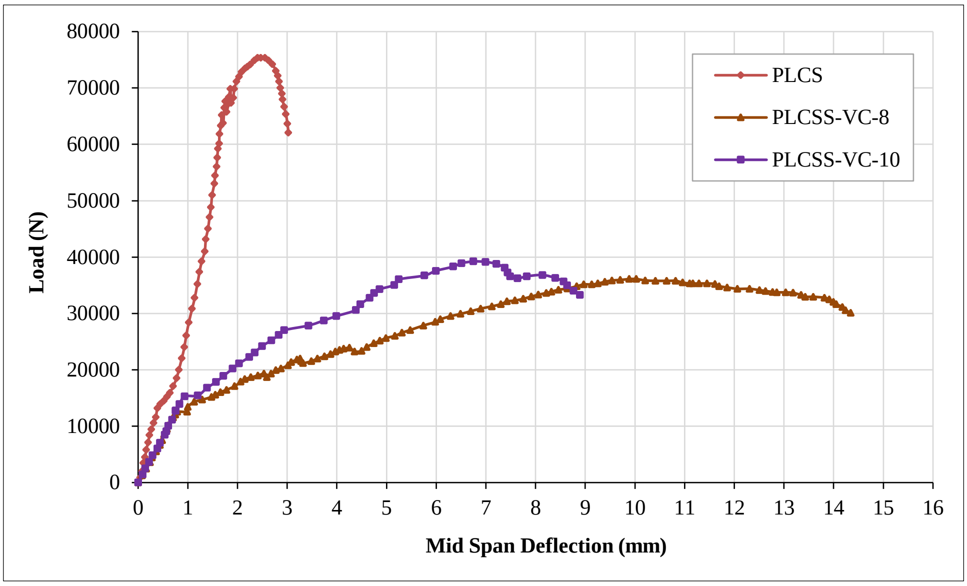

(b)

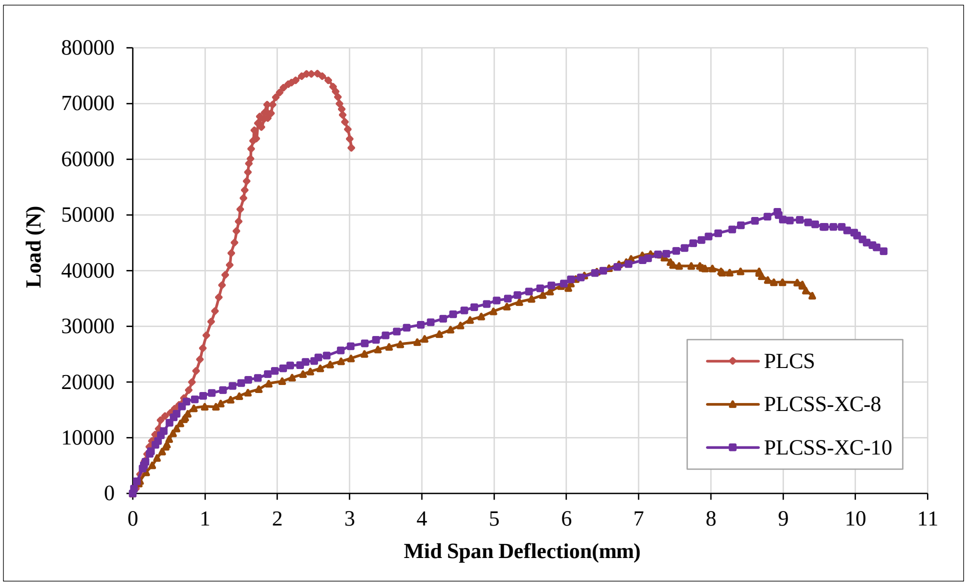

(c)

Figure 10. Effect of The Number and Layout of Shear Connectors on The Load- Deflection Curves for Specimens with (a) IC, (b) VC, and (c) XC in Comparison with PLCS

Table 3. Summary of Test Results

Specimen Ref.	First Crack Load $P_{cr,exp}$ (kN)	Deflection at First Crack Load $U_{cr,exp}$ (mm)	Elastic Stiffness $= \frac{P_{cr,exp}}{U_{cr,exp}}$ (N/mm)	Maximum Load Value (kN)	Moment Capacity (kN.m)	Midspan Deflection Value (mm)	Ductility $DI = \frac{U_{Ult}}{U_{cr}}$	Energy Dissipation (kN.mm)	Failure Mode[b]
PLCSS-NC[a]	4.1	0.96	4.3	12.3	1.8	22.8	23.7		
PLCS	13.2	0.39	34040.9	75.4	11.3	2.5	6.6	106	Flexural brittle
PLCSS-IC-10	11.3	0.93	12095.6	26.8	4.0	13.3	14.2	251.0	Flexural Tension
PLCSS-VC-10	15.3	0.94	16337.2	39.2	5.9	6.8	7.21	175.0	Shear at the bottom layer
PLCSS-XC-10	16.5	0.74	22291.2	50.5	7.6	8.9	12.0	280.4	Shear at top layer
PLCSS-IC-8	8.5	0.94	8957.6	22.7	3.4	19.6	20.7	323.8	Flexural Tension
PLCSS-VC-8	12.6	0.79	15893.5	36.1	5.4	10.0	12.7	248.3	Shear at the bottom layer
PLCSS-XC-8	15.3	0.84	18078.5	43.0	6.4	7.2	8.5	187.3	Shear at top layer

[a] The values for specimen PLCS-NC were calculated theoretically.

[b] The failure mode of the sandwich slabs that failed without forming a number of flexural cracks and whose failure is primarily due to the widening of the first cracks is classified as flexural brittle, while the failure mode of other sandwich slabs that failed by forming a number of flexural cracks are classified as flexural ductile.

3.2. Failure Modes of Panels

Different failure modes of the panels were identified, as shown in Figure 11. In PLCS, a louder sound and an increase in the width of one of the cracks that formed in the bottom of the slab were detected with a deflection that occurred immediately after the peak load, whereas the other cracks essentially stopped spreading. Then, the load was decreased pronouncedly with a slight increase in the value deflection (structural softening). The bond between the concrete and steel reinforcement is reduced because of the foamed concrete's porosity. At increasing load, the poor bonding accompanied by concrete deterioration near the reinforcement reduced the load transfer efficiency between the concrete and steel reinforcement, leading to brittle failure in the tension zone.

The flexural strength of solid concrete is higher than that of the sandwich slabs and is occupied by low deflection and energy absorption values. PLCSS-IC-8 and PLCSS-IC-10, flexural cracks were noticed at the front and bottom surfaces of the top and bottom concrete layers. These cracks in the pure bending zone propagated transversely across the layers, and these specimens experienced ductile flexural mode. The crack opening then widened. A louder sound could then be heard, and a compression fracture in the upper layer had started. The lower number of connectors will lead to low initial stiffness of the sandwich specimens. The sandwich slabs with V and X connectors failed by developing and widening the inclined shear cracks that tended to connect the loading point and nearest support in the constant shear region.

These cracks are formed at the cross-section where bending and shear stresses are significant. Hence, the failure of these panels may be attributed to the material failure of concrete due to mixed mode fracture conditions; in sandwich slabs with V-connectors, PLCSS-VC-8, and PLCSS-VC-10 failed in shear by forming inclined shear cracks in the bottom layers. In contrast, the specimens with X-connectors, PLCSS-XC-8 and PLCSS-XC-10, failed by forming inclined shear cracks in the top layer. It may be concluded that the flexural mode with a lower load in sandwich slabs with I connectors indicates that these connectors are unable to maintain a high degree of composite action after the elastic stage, resulting in poor shear transfer.

The layers begin to act independently, causing the flexural stress to dominate and reducing the panel stiffness and bending strength. In specimens with V and X connectors, the two types of connectors effectively transfer load due to the high degree of composite action, allowing them to withstand higher loads and put more demand on concrete shear strength, leading to shear failure. The concrete tensile strength and the section properties limited the concrete layer shear strength. All the sandwich slabs behaved as composite members until failure, and the reduction in stiffness after the cracking load was due to material strength limitation. Therefore, it may be concluded that the demountable steel shear connectors provide adequate shear capacity to achieve partial composite action of the sandwich slab.

(a)

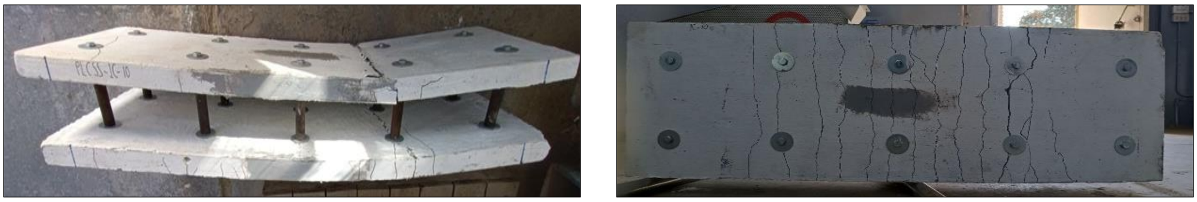

(b)

(c)

(d)

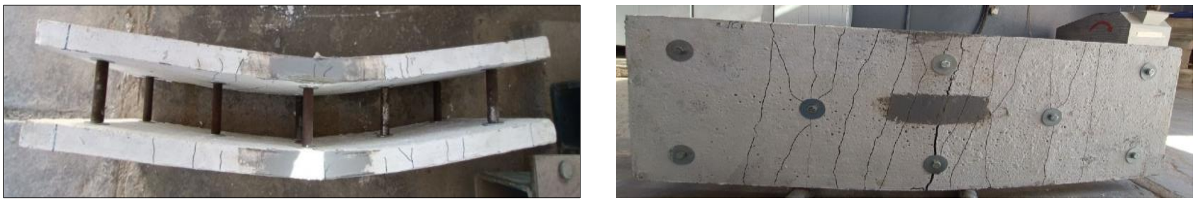

(e)

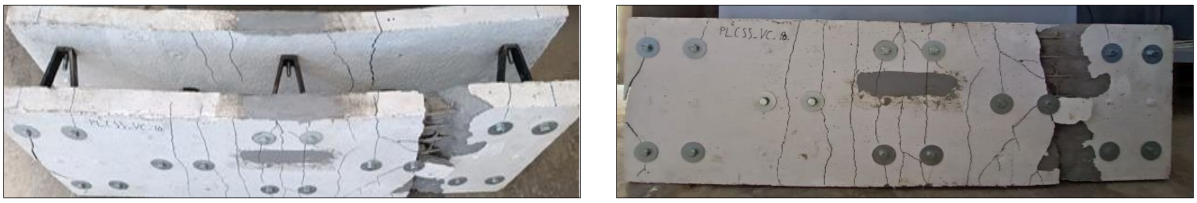

(f)

(g)

Figure 11. Crack Patterns at Side and Bottom View for: (a) PLCS ;(b) PLCSS-IC-10; (c) PLCSS-VC-10; (d) PLCSS-XC-10; (e) PLCSS-IC-8; (f) PLCSS-VC-8; (g) PLCSS-XC-8

3.3. Ductility

The ability of the structure to sustain plastic deformation before failure without losing its structural integrity is measured by the ductility index. The ductility values of the tested solid and sandwich slabs are calculated as the ratio of the ultimate to the yield's displacements [31, 43] and presented in Table 3 and Figure 12. The deformation capacity has also been evaluated regarding energy dissipation capacity by calculating the area under the load-deflection curve [31, 43] and are presented in Figure 13. Higher energy absorption means more plastic deformation before failure, making the panel more ductile. It could be observed that the PLCSS-IC-8 has the highest value of ductility because of the yielding of bolts in this specimen, which allowed a more significant displacement. The ductility value decreases with the increase in the number of connectors in panels with I and V connectors. In the specimen with fewer I and V connectors, each bolt must carry a greater portion of the applied load. The larger individual stress results in local yielding and progressive failure of the bolts. This gradual yielding offers higher ductility in the specimens. In contrast, the larger number of these connectors with uniform distribution causes a smaller amount of shear stress distributed uniformly in the bolts. The number of X connectors enhances the contribution to the improvement of flexural capacity and allows more displacement, which raises the ductility value.

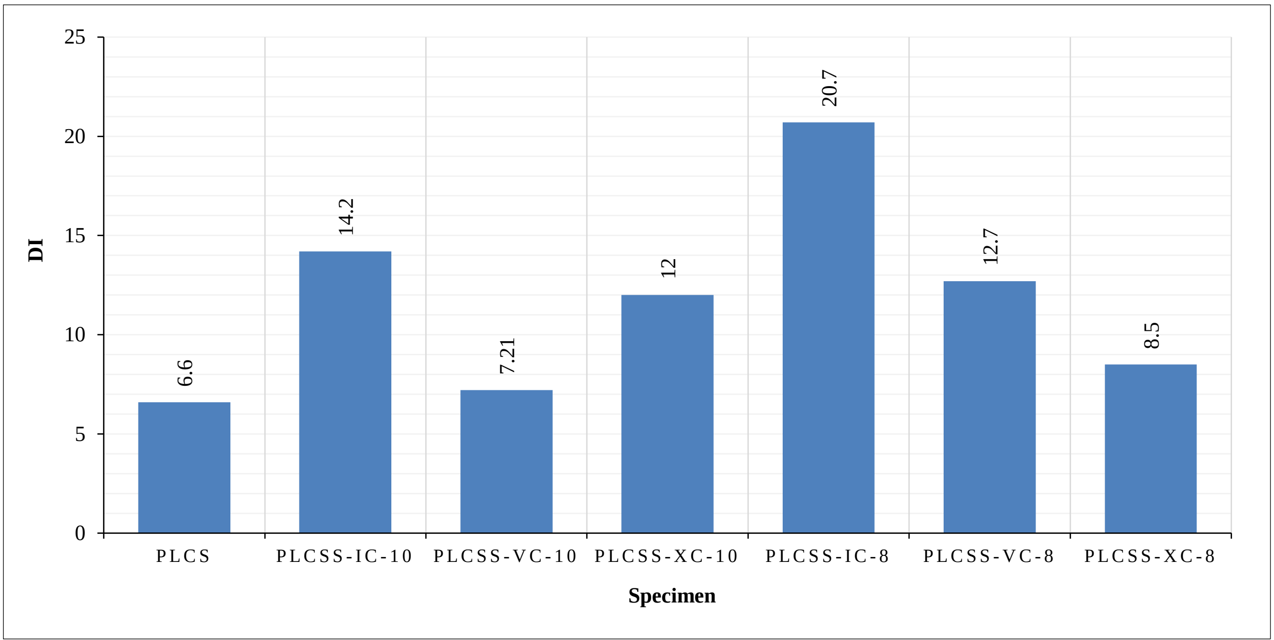

Figure 12. Ductility Index for The Tested Specimens

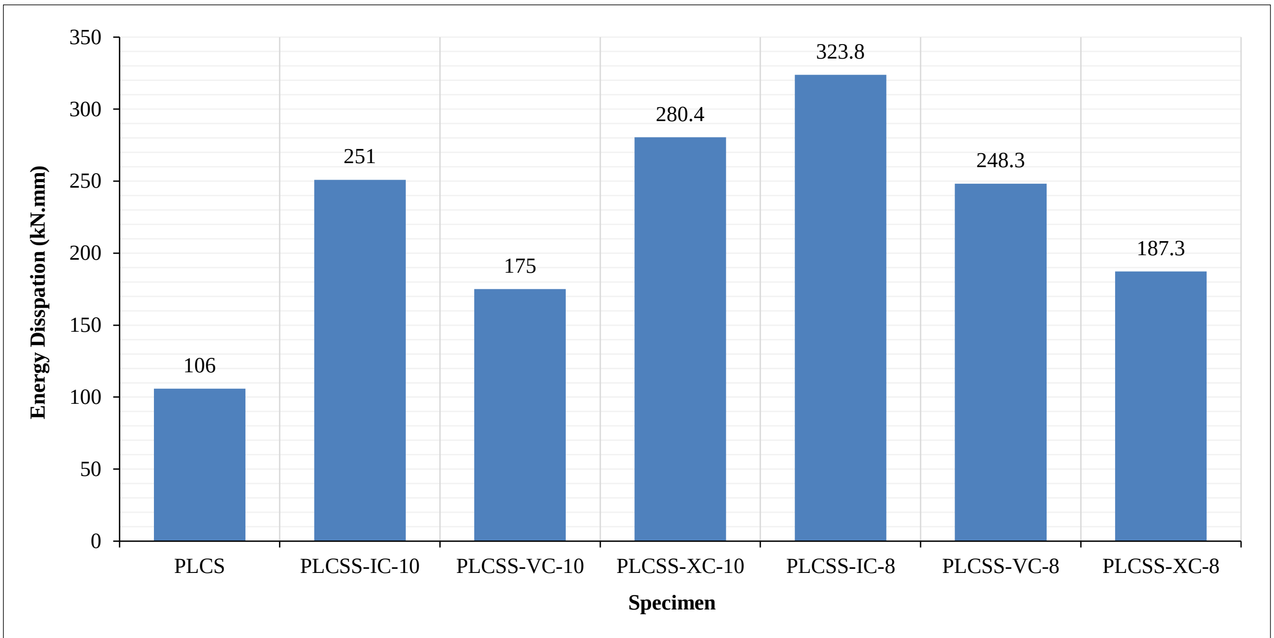

Figure 13. Energy Dissipation for The Tested Specimens

3.4. The Degree of Composite Action

A key consideration for sandwich panels is the degree of composite action (DCA), which is used as an index of connector performance. DCA attained by the tested sandwich slabs will be described in detail in this section, together with the flexural capacity and deflection of the full composite (FC) and non-composite (NC) of PLCS. The DCA is assessed considering both stiffness and strength parameters. The results of the degree of composite action are presented in Table 3. Various methods have evaluated the DCA using: section modulus and strain difference to find the moment of the panel [22, 44–46], the theoretical value of the moment of inertia [33, 47, 48], deflection at selected loads (deflection method) [2, 30, 49], the ultimate load (load method) [14], and strain (strain method) [50], and the neutral axis [51].

3.4.1. Flexural Strength Equations of Full and Non-Composite PLCSS

The flexural behaviour of non-composite and fully composite PLCSS is theoretically examined by the transformed section approach of the ACI318-19 Code to consider the degree of composite action. Both concrete layers function as a single structural unit when bending moment is applied to a full composite PLCSS. In contrast, in the non-composite PLCSS, the neutral axis is found within the thickness of each layer, and the flexural characteristics are easily calculated by adding the flexural strength of each individual layer. In this study, to directly compare the panels to theoretical calculations, a linear portion is assumed up to the first crack, and two states were considered to define the flexural behavior of BLCSS: the cracking and ultimate states.

M_{cr}, the first cracking moment, is calculated from Equation 1:

$$M_{cr} = \frac{f_r I_g}{y} \tag{1}$$

M_u, ultimate moment capacity is calculated from Equation 2

$$M_u = A_s f_y (d - \frac{a}{3}) \tag{2}$$

$$a = \frac{A_s f_y}{0.85 \acute{f}_c b} \tag{3}$$

where f_r is modulus of rupture obtained as $f_r = 0.62\lambda\sqrt{\acute{f}_c}$, $\lambda = 0.85$ (ACI-19), I_g is moment of inertia of the un-cracked section, y_t is distance from the neutral axis to the outer tensile face, A_s is entire area of reinforcement, f_y is yield stress of the reinforcement, d is effective depth of the panel, b is width of the panel.

The maximum deflection at mid-span for the non-composite panel is calculated from Equation 4:

$$\Delta_{max} = \frac{Pa}{12\,EI}(\frac{3}{4}L^2 - a^2) \tag{4}$$

where P is total applied load, a is distance between the support and point load, L is total span, E is modulus of elasticity, I is moment of inertia of the section.

The values of cracking load, mid span deflection at cracking load, ultimate load, and maximum mid span deflection for non-composite sandwich specimens (PLCSS-NC) are presented in Table 2.

3.4.2. Assessment of The Degree of Composite Action

The load-deflection response of the sandwich slab provides information about the degree of composite action. The bending stiffness and strength of partially composite panels lie between those of fully composite panels and non-composite panels [10]. The linear stage for each test panel is shown in Figure 14. The load-deflection curves of PLCS representing the full composite case and PLCSS-NC are added for reference. Evidently, every curve lies within the range between FC and NC.

Since the PLCSS-NC has the lowest cracking load value (4.1 kN), the experiment moment of inertia and DCA values are evaluated at this load for all the panel specimens for assessing DCA in the elastic region. The results of DCAs using the load, displacement, strain, and neutral axis methods are presented in Table 4.

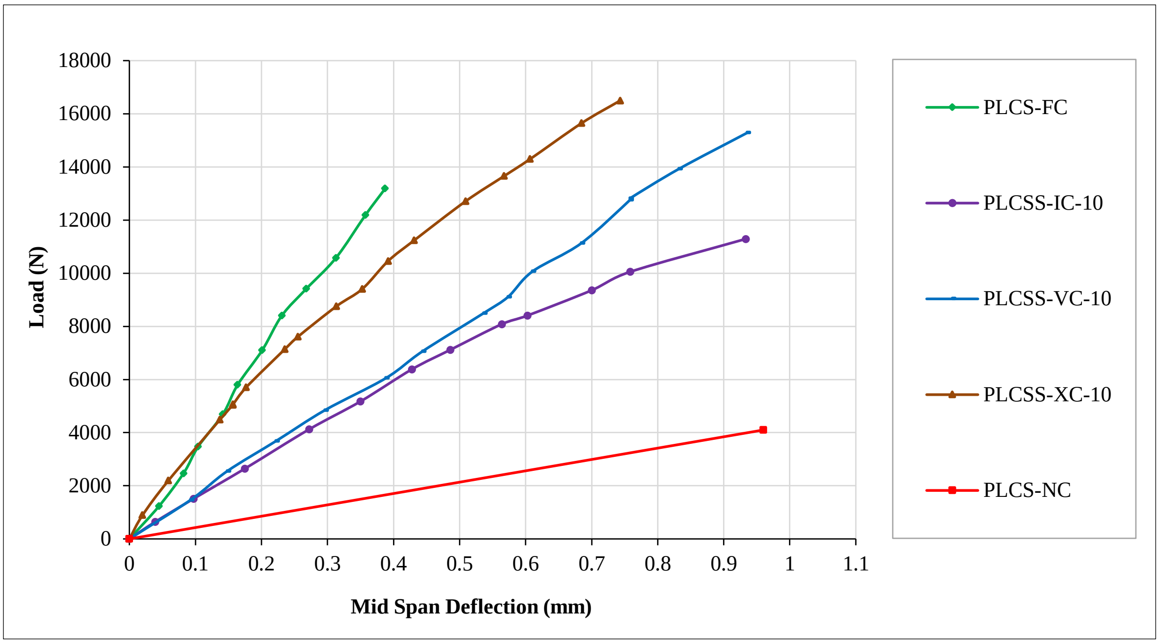

(a)

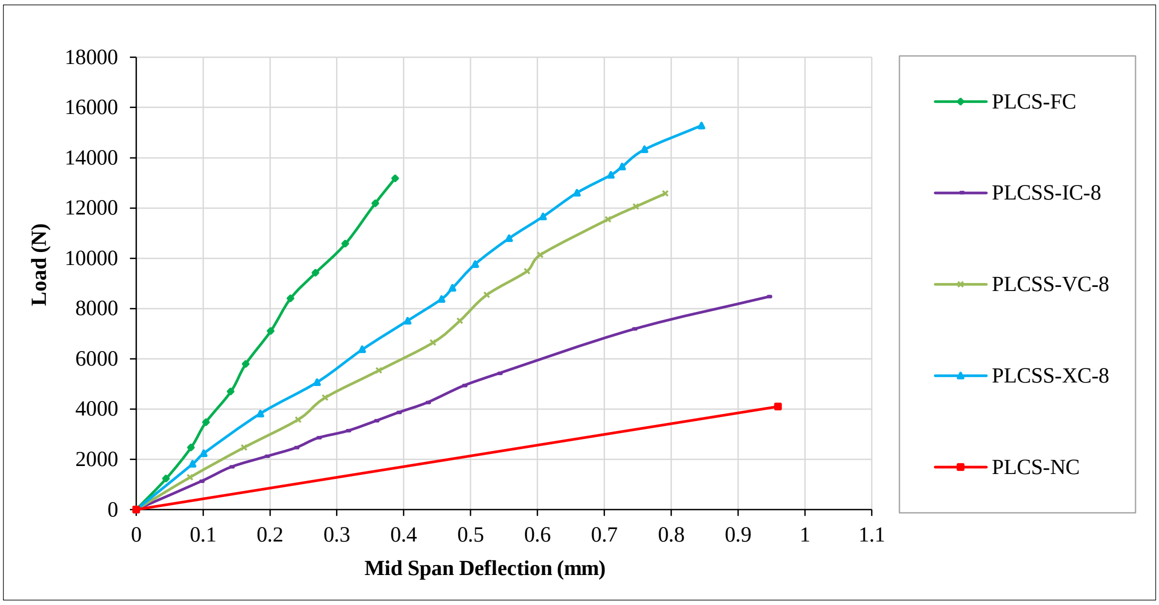

(b)

Figure 14. Comparing Stiffnesses of Test Specimens before the First Crack with Full Composite and Non-Composite Panels for (a) Group 2, and (b) Group 3

Table 4. Degree of Composite Action of the Tested Specimens

Specimen Ref.	DCA % by Load Method at cracking	DCA % by Load Method at Ultimate	I_{test} (mm^4) by Displacement Method at Selected Load=4.1 kN	DCA% by Displacement Method at Selected Load=4.1 kN	I_{test} (mm^4) by Strain Method at Selected Load=4.1 kN	DCA% by Strain Method at selected Load=4.1kN	DCA by Neutral Axis Method at selected Load=4.1kN
PLCS-NC	0	0	3821592	0	540000	0	0
PLCS	100	100	28855224.98	100	412745452	100	100
PLCSS-I-10	79.14	22.98	13557369.15	38.89	262053506	63.44	71.99
PLCSS-V-10	123.10	42.73	14758332.11	43.69	382599564	92.69	90.69
PLCSS-X-10	136.45	60.69	29603911.05	102.99	388698891	94.17	95.92
PLCSS-I-8	48.06	16.60	8781569.934	19.81	194892361	47.15	57.90
PLCSS-V-8	93.29	37.78	13780990.37	39.78	357264550	86.54	84.64
PLCSS-X-8	123.11	48.66	17926954.09	56.34	371018579	89.88	92.01

A. Load Method

The degree of composite action by load DCA_{Load} was evaluated at cracking and ultimate load using Equation 5 [22].

$$DCA_{Load} = \frac{P_{exp} - P_{NC}}{P_{FC} - P_{NC}} \tag{5}$$

where P_{exp} is the experimental load of the specimen, P_{FC} is the experimental load of the PLCS, P_{NC} is the theoretical load of noncomposite panel (PLCSS-NC) by using Equations 1 and 2.

B. Displacement Method

Within the stiffness approach is the displacement method. Initially, the degree of composite action in terms of initial stiffness was used to evaluate the PCSP composite action prior to cracking. The value could be calculated using the following equation proposed by Pessiki & Mlynarczyk [52]. This method can be applied to the elastic region before cracking.

$$DCA\ (100\%) = \frac{I_{test} - I_{NC}}{I_{FC} - I_{NC}} \times 100 \tag{6}$$

For a 4-point bending test under simply supported conditions, the moment of inertia is found using Equation 6 [37, 42, 53].

$$I_{test} = \frac{a\,K}{12E_c}\left(\frac{3}{4}L^2 - a^2\right) \tag{7}$$

K is calculated using Equation 7:

$$K = \frac{P}{\Delta} \tag{8}$$

where I_{exp} is moment of inertia that obtained from the load–displacement curve in the linear elastic stage, I_{NC} is theoretical value of the moment of inertia for a non-composite specimen (PLCSS-NC), I_{FC} is experimental value of the moment of inertia for a full composite panel (PLCS), L is span of the panel, a is the distance of the line load applied to the specimens from the support, P is the applied load on the panel, Δ is the deflection at mid-span.

C. Strain Method

The strain method, as provided by Equation 9 [48, 49, 52] uses the specimen's strain at the linear elastic stage for calculating I_{test}:

$$I_{test} = \frac{M\,h}{\sigma_{bot} - \sigma_{top}} = \frac{M\,h}{E(\varepsilon_{bot} - \varepsilon_{top})} \tag{9}$$

where M is midspan moment of the specimen, h is distance between the top and bottom surface, σ_{bot} is tensile stress of the concrete on the bottom surface of the specimen taken as a positive value and the concrete, σ_{top} is compressive stress on the top surface of the specimen taken as a negative value.

The strain data at (4.1 kN) presented in Figure 15 were used to compute DCA in the elastic stage for the sandwich slabs.

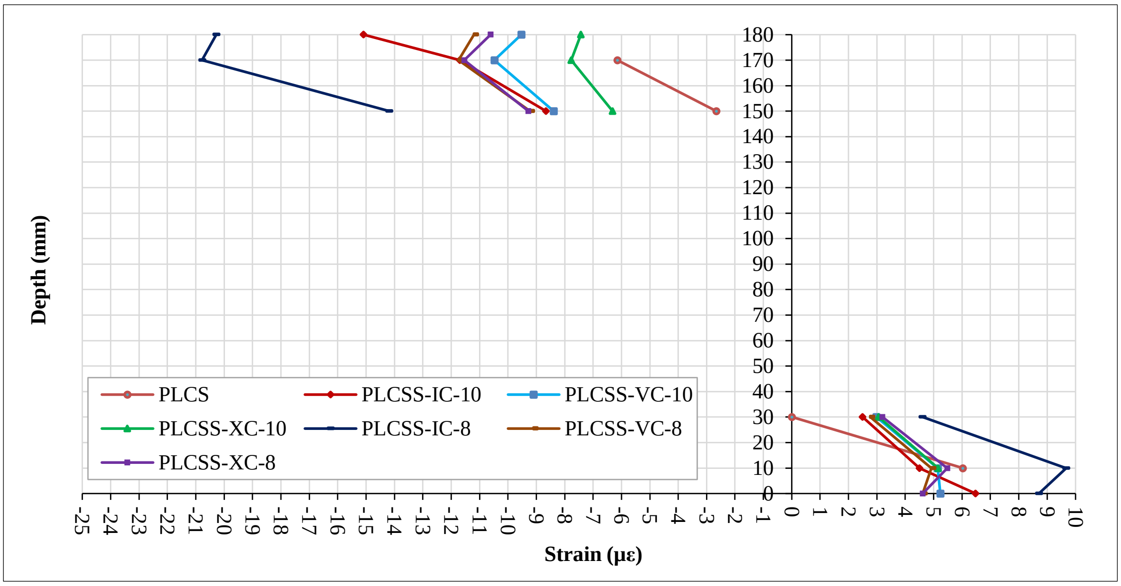

Figure 15. Strain Variation Across the Panel Depth for: (compression is negative)

D. Neutral Axis Method

The distance between the neutral axes of the inner and outer concrete wythes can be used to calculate the DCA of PLCSSs [50]. The DCA will be calculated from Equation 10.

$$DCA = \left(1 - \frac{X_{test}}{t - t_1}\right) \times 100 \tag{10}$$

where X_{test} is distances between the neutral axis of the inner and outer concrete wythes for the panels, t, t_1 is thicknesses of the total panel and inner and outer concrete wythes, respectively.

3.4.3. Comparison of the Four Methods

The results of the four methods used to calculate the DCA are shown in Figure 16. The lowest value of cracking load was found in PLCS-NC, this load was selected to calculate the DCA in the linear stage. Only the load method is applicable to calculate the DCA at the ultimate load.

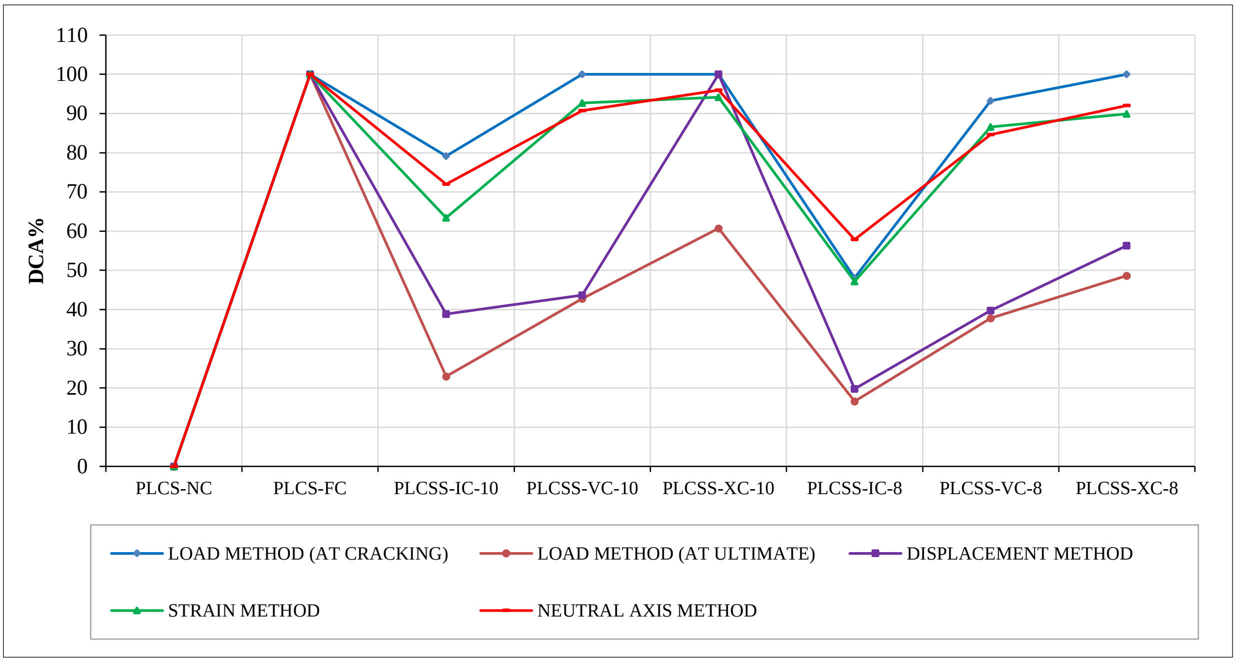

Figure 16. Comparison of Degree of Composite Action Calculated by Five Methods

In general, according to the load method, DCA decreases with the load applied after the cracking load due to the decrease in shear transferring capacity, which occurs due to the following: the yielding of the bolts in the sandwich slabs with I-connectors, which leads to increased slippage between their layers, the formation and widening of cracks primarily in the top and bottom layers, and the shear failure that occurred in the sandwich slabs with X and V connectors. DCA increases with the number of shear connectors at the elastic and ultimate elastic stages. Sandwich slabs with X-connectors scored on the largest value of DCA using the four methods. Each of the four methods produced a different DCA value. DCA values using the load method at cracking load were the highest in all sandwich slabs except PLCSS-IC-8 and decreased to their lowest when the displacement method was used. In PLCSS-XC-10, the displacement method showed the highest value of DCA in addition to the load method, and the lowest value was produced using the strain method. The results of the DCA were close using the strain and neutral axis methods in all sandwich slabs because of the similarity of the principle of the two methods in using the results of strain across the section. Notably, the strain method and the neutral axis exhibited similar results for high DCAs.

4. Applicability of PLCSS with Demountable Steel Shear Connectors to Roof and Floor Applications

The DCA presented in the previous section proved the efficiently of the bolted shear connectors in transferring shear between the layers of sandwich panels. Shear connectors helped the sandwich panels act as a unit to resist the bending moment. With a high degree of composite action, load capacity is higher.

ACI 318-19 specifies that a simply supported one-way slab must have a minimum thickness of L/20. As a result, the 180 mm depth of specimens considered in this study can have a span length of 3600 mm. Based on the moment capacity indicated in Table 3, the panels' maximum uniform loads can be calculated and compared to the load requirements of the appropriate building code. According to ACI 318-19, the roof and floor have L/360 and L/180 limits for instantaneous deflection due to live load. The maximum allowable deflection for the specified span is 3 mm based on the L/360 criteria. Based on the moment of inertia listed in Table 4, the load associated with the allowable sandwich panel's deflection is displayed in Table 5. The values listed below are based on the assumption that the section is uncracked. Table 5 shows that the maximum allowable load for each type is higher than the live load for most building applications (2.4-11.97 kPa) [54], so the PLCSS with demountable steel shear connectors can be used for roof and floor applications.

Table 5. Maximum Uniformly Distributed Loads Sustained by PLCSS Specimens

Ref	Based on strength (kPa)	Based on stiffness (kPa)
PLCSS-IC-10	26.54	48.73
PLCSS-VC-10	38.90	53.04
PLCSS-XC-10	50.14	106.40
PLCSS-IC-8	22.55	31.563
PLCSS-VC-8	35.80	49.53
PLCSS-XC-8	42.61	64.43

Table 6 compares the results of the sandwich slab BLCSS-XC-10 and previous studies of sandwich panels made with different types of concrete and steel connectors. Compared to the study by Alfeehan & Sheer [3], which used a similar technique in connecting the layers of the reactive powder concrete sandwich panel but with a higher number of stud connectors, typically BLCSS-XC-10, exhibited higher cracking and ultimate load capacity and lower deflection. Also, BLCSS-XC-10 had higher cracking and ultimate load than the sandwich panel in previous studies that used continuous steel truss connectors with foamed, normal, and self-compacting concrete. These results validated the suggested connectors' efficiency and effectiveness in producing integrity lightweight sandwich panels with simple connection characteristics.

Table 6. Comparison of Previous Studies with BLCSS-XC-10

Study	Dimensions	Thickness of layers	Type of connectors	Type of concrete	Number of connectors	Cracking load (kN)	Ultimate load (kN)	Ultimate deflection (mm)	*Difference in cracking load	*Difference in ultimate load	**Difference in ultimate deflection
[3]	980×420	40-30-40	Steel stud connectors with mechanical approach	Reactive powder concrete	11	12.5	52.5	14.09	19	-11.1	-58
	980×420	30-30-30	Steel stud connectors with mechanical approach	Reactive powder concrete	11	10.5	35	17.15	31.9	25.9	-92.7
	980×420	30-60-30	Steel stud connectors with mechanical approach	Reactive powder concrete	11	17.5	43.5	14.4	-13.4	7.9	-61.8
[55]	2000×750	40-30-40	Continuous double steel truss	Foamed concrete	Continuous connectors	5.1	25.63	22.1	91	85	-
[47]	2000×750	40-40-40	Continuous steel truss	Normal concrete	Continuous connectors	10.5	22	19	81.3	87.2	-
[56]	3000×1200	25-100-25	Continuous steel truss with concrete edge beam	Self-compacting concrete	Continuous connectors	9.7	20.4	30	92.8	95	-

* Cracking and ultimate load were calculated and compared per meter length (width=0.4 m)

** A deflection comparison was made only for shorter specimens than the specimens in the study.

5. Conclusions

In this paper, experimental and theoretical data of small-scale sandwich slabs have been presented to better understand the flexural behavior of precast lightweight concrete sandwich slabs with demountable steel shear connectors, particularly the role of the shear connectors in developing the efficient composite action in the sandwich slabs for the floor application. DCAs were calculated and compared using load, displacement, strain, and N.A. methods. Based on the findings of this study, the following conclusions can be presented:

- Fabricating sandwich panels with demountable steel shear connectors using the procedure presented in this paper is quick, simple, economical, and efficient. It provides good control on the thickness of panels by using connectors with the required depth and provides the possibility of replacing the damaged layers of the sandwich slabs with new ones. The demountable steel shear connectors with three bolts (V connector) and four bolts (X connector) used in this study contribute to increasing the flexural strength of the sandwich panels and transferring shear between the layers.
- In comparison to the solid slab, the reduction in the weight of the sandwich slab in this study is 55%, accompanied by a decrease in the strength equal to 33%, with the possibility of reducing this difference in strength by using concrete with higher strength or using a greater number of connectors.

- Crack patterns in the tested sandwich slabs appeared in one direction only, similar to solid one-way slabs. The behavior of all sandwich specimens tested is between the ideal behavior of full composite and nanocomposite. The degree of composite action in terms of ultimate load could be enhanced using concrete with higher strength. Sandwich stiffness is significantly affected by the type and number of demountable shear connectors. The total number of bolts used in the demountable steel shear connectors and the number of connectors significantly affect achieving structural efficiency and enhancing the composite action of sandwich specimens.
- Using V and X connectors enhances the composite action between layers, increasing the shear demand and making the shear failure more likely. It is necessary to optimize the design of the sandwich slab by determining the desired failure mode and load capacity by achieving a balance between the stiffness of the connector and the concrete layer capacity (increasing the thickness of the layer or using concrete with higher tensile strength).
- The sandwich slabs tested experienced large deformation prior to failure and showed a ductile behavior compared to the solid slab. The sandwich specimens PLCSS-IC-8 showed the highest energy dissipation capability (i.e. 325.76 kN.m) among all specimens, which indicates the ductility behavior is also the largest. Failure in the specimens with X and V connectors occurs in the concrete material, so using higher strength concrete with demountable shear connectors can increase the load capacity of the sandwich slabs. No bolt failure could be observed at the end of the test.
- The load, strain, and neutral axes methods provide close results in predicting the DCAs; on the other hand, the displacement method provides low values of DCAs, which can be used as a conservative method in designing sandwich panels with demountable shear connectors.
- Based on the strength and immediate deflection criteria, the PLCSS with demountable steel shear connectors can be used for roof and floor applications.

The test results of this study prove the efficiency of the demountable shear connectors in achieving the desired objectives in the service loading condition and may change the failure mode from brittle to flexural when using the required concrete strength and necessary number of connectors. Based on these results, PLCSS with demountable steel shear connectors may serve as an alternative to the solid concrete slabs in the buildings. Further investigations are recommended for two-way slabs under different loading conditions.

6. Declarations

6.1. Author Contributions

Conceptualization, R.H.A., S.A.O., A.W.A., and A.N.H.; methodology, R.H.A., S.A.O., A.W.A., and A.N.H.; validation, R.H.A.; formal analysis, R.H.A.; investigation, R.H.A.; resources, R.H.A.; data curation, R.H.A.; writing—original draft preparation, R.H.A.; writing—review and editing, S.A.O., A.W.A., and A.N.H.; visualization, R.H.A.; supervision, S.A.O., A.W.A., and A.N.H.; project administration, R.H.A., S.A.O., A.W.A., and A.N.H.; funding acquisition, R.H.A. All authors have read and agreed to the published version of the manuscript.

6.2. Data Availability Statement

The data presented in this study are available in the article.

6.3. Funding

The authors received no financial support for the research, authorship, and/or publication of this article.

6.4. Acknowledgements

The authors would like to thank Al-Mustansiriyah University, Iraq; University Kebangsaan Malaysia (UKM), Malaysia; Alturath University, Iraq; and Baghdad University, Iraq, for supporting this work.

6.5. Conflicts of Interest

The authors declare no conflict of interest.

7. References

[1] Einea, A., Salmon, D. C., Fogarasi, G. J., Culp, T. D., & Tadros, M. K. (1991). State-of-the-art of Precast Concrete Sandwich Panels. PCI Journal, 36(6), 78–92. doi:10.15554/pcij.11011991.78.98.

[2] Daniel Ronald Joseph, J., Prabakar, J., & Alagusundaramoorthy, P. (2017). Precast concrete sandwich one-way slabs under flexural loading. Engineering Structures, 138, 447–457. doi:10.1016/j.engstruct.2017.02.033.

[3] Alfeehan, A. A., & Sheer, N. M. (2018). Reactive powder concrete sandwich panels with mechanical connection approach. 2018 International Conference on Advance of Sustainable Engineering and Its Application (ICASEA), 121–125. doi:10.1109/icasea.2018.8370968.

[4] Alabduljabbar, H., Alyousef, R., & Amran, M. (2019). Applicable use of lightweight foam concrete composite sandwich panels as a flooring system. Sustainable Construction Materials and Technologies (SCMT), 1, 9–19. doi:10.18552/2019/idscmt5002.

[5] Sumadi, S. R., & Ramli, M. (2008). Development of lightweight ferrocement sandwich panels for modular housing and industrialized building system. Universiti Teknologi Malaysia (UTM), Research Vote, 73311.

[6] Chen, Y., Kang, C., Wu, Y., & Qian, Z. (2022). Bending Performance of Precast Ceramsite-Concrete-Insulated Sandwich Panel with Stainless Steel Shear Connectors. Buildings, 12(10). doi:10.3390/buildings12101640.

[7] Lou, X., Xue, W., Bai, H., Li, Y., & Huang, Q. (2022). Shear behavior of stainless-steel plate connectors for insulated precast concrete sandwich panels. Structures, 44, 1046–1056. doi:10.1016/j.istruc.2022.08.073.

[8] Guerrero, N., Carrillo, J., Herrera, R. I., & Marante, M. E. (2024). Experimental and numerical investigation on the behavior of concrete sandwich slab panel for a structural system. Journal of Building Engineering, 86. doi:10.1016/j.jobe.2024.108930.

[9] Egbon, B., & Tomlinson, D. (2021). Experimental investigation of longitudinal shear transfer in insulated concrete wall panels with notched insulation. Journal of Building Engineering, 43. doi:10.1016/j.jobe.2021.103173.

[10] Huang, J., Jiang, Q., Chong, X., Ye, X., & Wang, D. (2020). Experimental study on precast concrete sandwich panel with cross-shaped GFRP connectors. Magazine of Concrete Research, 72(3), 149–162. doi:10.1680/jmacr.18.00258.

[11] Chen, A., Yossef, M., & Hopkins, P. (2020). A comparative study of different methods to calculate degrees of composite action for insulated concrete sandwich panels. Engineering Structures, 212. doi:10.1016/j.engstruct.2020.110423.

[12] Chen, D., Li, K., Yuan, Z., Cheng, B., & Kang, X. (2022). Shear Behavior of FRP Connectors in Precast Sandwich Insulation Wall Panels. Buildings, 12(8). doi:10.3390/buildings12081095.

[13] Huang, J. Q., & Dai, J. G. (2020). Flexural performance of precast geopolymer concrete sandwich panel enabled by FRP connector. Composite Structures, 248. doi:10.1016/j.compstruct.2020.112563.

[14] Tomlinson, D., & Fam, A. (2015). Flexural behavior of precast concrete sandwich wall panels with basalt FRP and steel reinforcement. PCI Journal, 60(6), 51–71. doi:10.15554/pcij.11012015.51.71.

[15] Liu, X., Wang, X., Yang, T., & Wu, Z. (2022). The Shear Behavior of Insulated Precast Concrete Sandwich Panels Reinforced with BFRP. Buildings, 12(9). doi:10.3390/buildings12091326.

[16] Jiang, H., Guo, Z., Liu, J., & Liu, H. (2018). The Shear Behavior of Precast Concrete Sandwich Panels with W-shaped SGFRP Shear Connectors. KSCE Journal of Civil Engineering, 22(10), 3961–3971. doi:10.1007/s12205-018-0809-9.

[17] Einea, A., David C. Salmon, D. C., Tadros, M. K., & Culp, T. (1994). A New Structurally and Thermally Efficient Precast Sandwich Panel System. PCI Journal, 39(4), 90–101. doi:10.15554/pcij.07011994.90.101.

[18] Henin, E., Morcous, G., & Tadros, M. K. (2014). Precast/Prestressed Concrete Sandwich Panels for Thermally Efficient Floor/Roof Applications. Practice Periodical on Structural Design and Construction, 19(3). doi:10.1061/(asce)sc.1943-5576.0000213.

[19] Choi, K. B., Choi, W. C., Feo, L., Jang, S. J., & Yun, H. Do. (2015). In-plane shear behavior of insulated precast concrete sandwich panels reinforced with corrugated GFRP shear connectors. Composites Part B: Engineering, 79, 419–429. doi:10.1016/j.compositesb.2015.04.056.

[20] Mohamad, N., Khalifa, H., Abdul Samad, A. A., Mendis, P., & Goh, W. I. (2016). Structural performance of recycled aggregate in CSP slab subjected to flexure load. Construction and Building Materials, 115, 669–680. doi:10.1016/j.conbuildmat.2016.04.086.

[21] Zhang, M., Feng, W., Chen, K., & Li, B. (2024). Flexural Behavior of a New Precast Insulation Mortar Sandwich Panel. Applied Sciences, 14(5), 2071. doi:10.3390/app14052071.

[22] Cox, B., Syndergaard, P., Al-Rubaye, S., Pozo-Lora, F. F., Tawadrous, R., & Maguire, M. (2019). Lumped GFRP star connector system for partial composite action in insulated precast concrete sandwich panels. Composite Structures, 229. doi:10.1016/j.compstruct.2019.111465.

[23] Sevil Yaman, T., & Lucier, G. (2023). Shear Transfer Mechanism between CFRP Grid and EPS Rigid Foam Insulation of Precast Concrete Sandwich Panels. Buildings, 13(4). doi:10.3390/buildings13040928.

[24] Shin, D. H., & Kim, H. J. (2020). Composite effects of shear connectors used for lightweight-foamed-concrete sandwich wall panels. Journal of Building Engineering, 29. doi:10.1016/j.jobe.2019.101108.

[25] Huang, J. Q., & Dai, J. G. (2019). Direct shear tests of glass fiber reinforced polymer connectors for use in precast concrete sandwich panels. Composite Structures, 207, 136–147. doi:10.1016/j.compstruct.2018.09.017.

[26] He, Z. Z., Pan, P., Xiao, G. Q., Shen, S. D., & Ren, J. Y. (2022). Test and analysis on axial performances of GFRP restraint connectors for sandwich insulation wall panels. Journal of Building Engineering, 45, 103457. doi:10.1016/j.jobe.2021.103457.

[27] O'Hegarty, R., Kinnane, O., Grimes, M., Newell, J., Clifford, M., & West, R. (2021). Development of thin precast concrete sandwich panels: Challenges and outcomes. Construction and Building Materials, 267, 120981. doi:10.1016/j.conbuildmat.2020.120981.

[28] Tawil, H., Tan, C. G., Ramli Sulong, N. H., Nazri, F. M., Shamsudin, M. F., & Muhamad Bunnori, N. (2024). Optimization of Shear Resistance in Precast Concrete Sandwich Wall Panels Using an S-Type Shear Connector. Buildings, 14(6). doi:10.3390/buildings14061725.

[29] Goudarzi, N., Korany, Y., Adeeb, S., & Cheng, R. (2016). Characterization of the shear behavior of Z-shaped steel plate connectors used in insulated concrete panels. PCI Journal, 61(2), 23–37. doi:10.15554/pcij.03012016.23.37.

[30] Chen, A., Norris, T. G., Hopkins, P. M., & Yossef, M. (2015). Experimental investigation and finite element analysis of flexural behavior of insulated concrete sandwich panels with FRP plate shear connectors. Engineering Structures, 98, 95–108. doi:10.1016/j.engstruct.2015.04.022.

[31] Bishnoi, U., Danie Roy, A. B., & Kwatra, N. (2021). Out of plane performance of novel concrete sandwich panel using different geosynthetics. Construction and Building Materials, 300. doi:10.1016/j.conbuildmat.2021.124186.

[32] Gombeda, M. J., Naito, C. J., & Quiel, S. E. (2020). Development and performance of a ductile shear tie for precast concrete insulated wall panels. Journal of Building Engineering, 28. doi:10.1016/j.jobe.2019.101084.

[33] O′Hegarty, R., West, R., Reilly, A., & Kinnane, O. (2019). Composite behaviour of fibre-reinforced concrete sandwich panels with FRP shear connectors. Engineering Structures, 198. doi:10.1016/j.engstruct.2019.109475.

[34] Wang, W., Zhang, X. D., Zhou, X. L., Wu, L., & Zhu, H. J. (2021). Study on Shear Behavior of Multi-Bolt Connectors for Prefabricated Steel–Concrete Composite Beams. Frontiers in Materials, 8. doi:10.3389/fmats.2021.625425.

[35] Fang, Z., Liang, W., Fang, H., Jiang, H., & Wang, S. (2021). Experimental investigation on shear behavior of high-strength friction-grip bolt shear connectors in steel-precast UHPC composite structures subjected to static loading. Engineering Structures, 244. doi:10.1016/j.engstruct.2021.112777.

[36] Wang, W., Zhang, X. D., Ding, F. X., & Zhou, X. L. (2021). Finite element analysis on shear behavior of high-strength bolted connectors under inverse push-off loading. Energies, 14(2). doi:10.3390/en14020479.

[37] Zhang, Y., Zhang, J., Chen, B., & Zhang, Y. (2022). Shear Mechanism of High-Strength-Friction-Grip Bolts in Steel and Steel-Fiber-Reinforced-Concrete Composite Beams. Frontiers in Materials, 9. doi:10.3389/fmats.2022.899112.

[38] Luo, Y. B., Sun, S. K., Yan, J. B., Zhao, Y. C., & Lam, D. (2022). Shear Behavior of Novel Demountable Bolted Shear Connector for Prefabricated Composite Beam. Advanced Steel Construction, 18(4), 745–752. doi:10.18057/IJASC.2022.18.4.2.

[39] Abdulkareem, T., & A. Alfeehan, A. (2018). Effect of the Rib Depth to the Overall Beam Depth Ratio in the Lightweight One-Way Ribbed Slabs. International Journal of Engineering & Technology, 7(4.20), 438–442. doi:10.14419/ijet.v7i4.20.26239.

[40] Iraq Specifications No.45. (2021). Aggregate from Natural Sources for Concrete. Iraqi Ministry of Planning, Baghdad, Iraq.

[41] ASTM A1064/A1064M-18a. (2022). Standard Specification for Carbon-Steel Wire and Welded Wire Reinforcement, Plain and Deformed, for Concrete. ASTM International, Pennsylvania, United States. doi:10.1520/A1064_A1064M-18A

[42] ASTM F593-17. (2023). Standard Specification for Stainless Steel Bolts, Hex Cap Screws, and Studs. ASTM International, Pennsylvania, United States. doi:10.1520/F0593-17.

[43] Bastin, D. R. A., & Sharma, U. K. (2017). A study on different techniques of restoration of fire damaged reinforced concrete flexural members. Journal of Structural Fire Engineering, 8(2), 131–148. doi:10.1108/JSFE-03-2017-0026.

[44] Tomlinson, D., & Fam, A. (2018). Axial load-bending moment-interaction diagram of partially composite precast concrete sandwich panels. ACI Structural Journal, 115(6), 1515–1528. doi:10.14359/51710834.

[45] Al-Rubaye, S., Sorensen, T., Thomas, R. J., & Maguire, M. (2019). Generalized beam–spring model for predicting elastic behavior of partially composite concrete sandwich wall panels. Engineering Structures, 198. doi:10.1016/j.engstruct.2019.109533.

[46] Bush, T. D., & Stine, G. L. (1994). Flexural Behavior of Composite Precast Concrete Sandwich Panels with Continuous Truss Connectors. PCI Journal, 39(2), 112–121. doi:10.15554/pcij.03011994.112.121.

[47] Benayoune, A., Samad, A. A., Trikha, D. N., Ali, A. A., & Ellinna, S. H. M. (2008). Flexural behaviour of pre-cast concrete sandwich composite panel–experimental and theoretical investigations. Construction and Building Materials, 22(4), 580-592. doi:10.1016/j.conbuildmat.2006.11.023.

[48] Choi, I., Kim, J. H., & Kim, H. R. (2015). Composite behavior of insulated concrete sandwich wall panels subjected to wind pressure and suction. Materials, 8(3), 1264–1282. doi:10.3390/ma8031264.

[49] Frankl, B. A., Lucier, G. W., Hassan, T. K., & Rizkalla, S. H. (2011). Behavior of precast, prestressed concrete sandwich wall panels reinforced with CFRP shear grid. PCI Journal, 56(2), 42–54. doi:10.15554/pcij.03012011.42.54.

[50] Lorenz, R. F., & Stockwell, F. W. (1984). Concrete Slab Stresses in Partial Composite Beams and Girders. Engineering Journal, 21(3), 185–188. doi:10.62913/engj.v21i3.419.

[51] Zheng, T., Ge, Q., Xiong, F., Li, G., Xue, Y., & Deng, X. (2023). Study of the flexural performance and a novel calculation formula for the degree of composite action for precast concrete sandwich panels. Structural Design of Tall and Special Buildings, 32(18). doi:10.1002/tal.2065.

[52] Pessiki, S., & Mlynarczyk, A. (2003). Experimental evaluation of the composite behavior of precast concrete sandwich wall panels. PCI Journal, 48(2), 54–71. doi:10.15554/pcij.03012003.54.71.

[53] Jiang, H., Guo, Z., & Liu, J. (2018). Composite Behavior of Sandwich Panels with W-Shaped SGFRP Connectors. KSCE Journal of Civil Engineering, 22(5), 1889–1899. doi:10.1007/s12205-017-2050-3.

[54] ASCE/SEI 7-16. (2017). Minimum Design Loads and Associated Criteria for Buildings and Other Structures (7-16). American Society of Civil Engineers (ASCE), Reston, United States. doi:10.1061/9780784414248.

[55] Mohamad, N., Khalil, A. I., Abdul Samad, A. A., & Goh, W. I. (2014). Structural behavior of precast lightweight foam concrete sandwich panel with double shear truss connectors under flexural load. ISRN Civil Engineering, 317941. doi:10.1155/2014/317941.

[56] Daniel Ronald Joseph, J., Prabakar, J., & Alagusundaramoorthy, P. (2019). Experimental study on the flexural behavior of insulated concrete sandwich panels with wires as shear connectors. Alexandria Engineering Journal, 58(3), 901–908. doi:10.1016/j.aej.2019.08.005.